Scaling of pressure drop for oscillatory flow through a slot

Reni Raju
Department of Mechanical and Aerospace Engineering, The George Washington University, Washington, DC 20052, USA

Quentin Gallas[a)]
Department of Mechanical Engineering, University of Florida, Gainesville, Florida 32611, USA

Rajat Mittal[b)]
Department of Mechanical and Aerospace Engineering, The George Washington University, Washington, DC 20052, USA

Louis Cattafesta
Department of Mechanical Engineering, University of Florida, Gainesville, Florida 32611, USA

(Received 24 January 2007; accepted 15 May 2007; published online 23 July 2007)

Reduced-order modeling and design of zero-net mass-flux actuators require an understanding of several fundamental flow mechanisms governing the performance of these devices. One such aspect is the pressure drop due to oscillatory flow through a slot. In this Brief Communication, we use numerical simulations and experiments to examine physics-based scaling laws for the various mechanisms that determine the net pressure drop, and critically evaluate a proposed phenomenological model for predicting the nonlinear component of the pressure drop in oscillatory slot flows. © *2007 American Institute of Physics*. [DOI: 10.1063/1.2749814]

Zero-net mass-flux (ZNMF), or synthetic jet, actuators, are suitable for a range of applications including thrust vectoring, active control of separation, and drag reduction in a turbulent boundary layer.[1] They impart momentum to the external flow through an orifice or slot without any net addition of mass due to time periodic changes in the volume of a cavity via a driver. ZNMF actuators are therefore capable of providing unsteady forcing without any complex fluid circuitry and, by altering the actuation parameters, can be adapted to a variety of flow configurations.

Since the performance of these devices depends on several geometrical, structural, and flow parameters,[1–3] scaling laws are needed to quantify these dependencies. Furthermore, due to the range of scales involved, inclusion of a high-fidelity model[4] of a ZNMF actuator within a macroscale computational flow model turns out to be an expensive, if not prohibitive, proposition. Hence, simple but accurate models are required to predict the performance of these devices. Lumped-element models (LEMs) are one such class of reduced-order models where the actuator components are represented as elements in an equivalent circuit using conjugate power variables.[3,5,6] These models have been found to predict the general behavior of ZNMF actuators with reasonable accuracy. However, one major shortcoming remains the lack of a quantitative understanding of the unsteady flow physics in the orifice/slot.

The formulation of LEMs hinges on accurate prediction of the acoustic impedance, which is defined as the complex ratio of the pressure drop across the slot to the volume flow rate, $\Delta P/Q$ (Ref. 7). A steady laminar flow through a pipe/channel suffers linear "major" losses due to friction, and nonlinear "minor" losses due to entrance or exit flow. Similarly, for unsteady, fully developed laminar flow driven by an oscillatory pressure gradient, it is possible to calculate the linear complex flow impedance analytically.[8] However, due to the relatively short slot lengths in ZNMF actuators, the nonlinear minor losses associated with entrance and exit effects are expected to be important, and therefore, development of accurate predictive models for these losses will improve the fidelity of existing LEMs.[6]

In this Brief Communication, we use a control volume analysis to characterize the mechanisms governing the pressure drop across a finite-length channel with oscillatory flow, a configuration which is representative of a flow in the rectangular slot of a ZNMF jet.[6,13] Numerical simulations and experimental data are used to explore scaling laws for the various components of the pressure drop. A phenomenological model for the nonlinear minor losses, with potential application to the LEM, is also proposed and examined using the data from the numerical simulations.

Figure 1 shows a schematic of a ZNMF actuator slot of length h and depth d. The slot flow can generally be divided into *entrance*, *exit*, and fully developed *core* regions. If one defines the average stroke length for the slot flow as $L_0 = 1/d\int_0^{T/2} Q(t)dt$,[9] where T is the period of oscillation and $Q(t)$ is the instantaneous volume flux per unit span, then for the situation where $L_0/h \ll 1$, the entrance effects are expected to be small since the slot is much longer than the convective length scale of the slot flow. Thus, for this case, major losses corresponding to the fully developed flow in the slot are expected to be dominant. Conversely, for $L_0/h \gg 1$, the nonlinear entrance losses will be significant. In the intermediate $L_0/h \sim O(1)$ case, both loss mechanisms may be significant.

With the background provided in the previous para-

[a)]Present address: RENAULT - Research Department, 1 av. du Golf, 78288 Guyancourt Cedex, France.
[b)]Author to whom correspondence should be addressed.

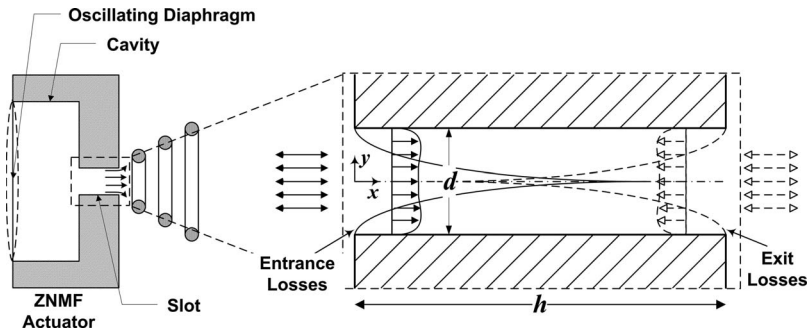

FIG. 1. Schematic of oscillatory flow in the slot of a ZNMF actuator.

graphs, we begin with a control volume analysis of the unsteady, pressure-driven *incompressible*, *laminar*, oscillatory flow in a rectangular slot with volume $\forall$. Mass conservation implies that $Q(t)$ is the same throughout the slot and therefore independent of the x location. Integrating the streamwise momentum equation over a unit span control volume extending from $0 \rightarrow x$ (Ref. 10) leads to

$$(\bar{p}_0 - \bar{p}_x)d = \rho x \frac{\partial Q}{\partial t} + \int_0^x \tau_w(x)dx + \rho \int_{-d/2}^{d/2} (u_x^2 - u_0^2)dy, \qquad (1)$$

where ρ is the density, $\bar{p}$ is the section averaged pressure, τ_w is the wall shear stress, and u is the streamwise (x) velocity. For a sinusoidal oscillation with angular frequency ω, i.e., $Q(t) = Q_{\max}\sin(\omega t)$, the dimensionless, time-dependent form of the above equation evaluated at the exit $(x=h)$ is

$$\Delta C_p = (\bar{p}_0 - \bar{p}_h)/q_j = \underbrace{\pi\left(St\frac{h}{d}\right)\cos(\omega t)}_{\Delta C_{p-\text{unsteady}}} + \underbrace{\int_0^{h/d} C_f d\left(\frac{x}{d}\right)}_{\Delta C_{p-\text{shear}}} + \underbrace{2\int_{-1/2}^{1/2}\left(\frac{u_h^2 - u_0^2}{\bar{U}_j^2}\right)d\left(\frac{y}{d}\right)}_{\Delta C_{p-\text{mom}}}, \qquad (2)$$

where $\bar{U}_j = 2/Td\int_0^{T/2} Q(t)dt$ is the time- and spatial-averaged expulsion velocity. Furthermore, $St = \omega d/\bar{U}_j$ is the Strouhal number, $C_f = \tau_w/q_j$ is the skin friction coefficient, and $q_j = 0.5\rho\bar{U}_j^2$. The contributions to the pressure drop are identified as follows: (a) $\Delta C_{p-\text{unsteady}}$: unsteady, linear inertia term; (b) $\Delta C_{p-\text{shear}}$: viscous loss; and (c) $\Delta C_{p-\text{mom}}$: nonlinear minor loss.

Attempts have been made to examine Eq. (2) via experiments.[5,6] The ZNMF actuator in experiments consists of a piezoelectric diaphragm mounted on the side of a U-shaped cavity and an axisymmetric cylindrical orifice. The relevant dimensionless parameters are the jet Reynolds number, $\text{Re}_j = \bar{U}_j d/\nu$, and the Stokes number, $S = \sqrt{\omega d^2}/\nu$, where ν is the kinematic viscosity. Note that the following holds: $(1/St) \equiv (L_0/\pi d) \equiv (\text{Re}_j/S^2)$ (Ref. 2) and all these parameters can be controlled by varying the amplitude of the actuator drive signal and the oscillation frequency.

The experiments allow for phase-averaged measurements of the exit velocity profile $u_h(y,t)$, which is used to estimate $\bar{U}_j$, and pressure on the internal cavity wall (denoted by p_c). The pressure drop $(\bar{p}_0 - \bar{p}_h)$ is then estimated as $(p_c - p_\infty)$, where p_∞ is the ambient pressure outside the cavity. It should be noted that depending on the jet configuration $(p_c - p_\infty)$ may overestimate $(\bar{p}_0 - \bar{p}_h)$ (Ref. 6). On the right-hand side (RHS) of Eq. (2), the first term, $\Delta C_{p-\text{unsteady}}$, is linear and only requires knowledge of St and h/d. On the other hand, $\Delta C_{p-\text{shear}}$ cannot be estimated in the experiments since it requires measurement of the time-dependent shear stress on the slot walls. Similarly, since $u_0(y,t)$, the velocity profile at the internal slot entrance, cannot be measured, it is not possible to estimate the last term, $\Delta C_{p-\text{mom}}$ with certainty. However, despite these experimental limitations, it is useful to examine the variation in the pressure loss, as estimated above, as a function of the key parameters of the jet.

Figure 2 shows the experimental ΔC_p for various cases as a function of $(St \cdot h/d)$. Despite the experimental uncertainty inherent in this pressure drop estimate, the data exhibits a linear trend at high $(St \cdot h/d)$. This indicates the dominance of the unsteady term in Eq. (2) at high $(St \cdot h/d)$. However, the data deviate from a linear trend at lower values of $(St \cdot h/d)$, which is indicative of significant contributions from the remaining terms in Eq. (2) (Ref. 5). Note that low values of $(St \cdot h/d)$ also usually correspond to cases where strong jets are formed,[2] and thus the simple linear model fails precisely for the conditions that are especially important in the context of active flow control. Better models for scaling the individual components of the pressure losses are therefore needed, and this is the motivation of the current study. Due to experimental limitations outlined above, the study of the contribution of the individual terms to ΔC_p is best ac-

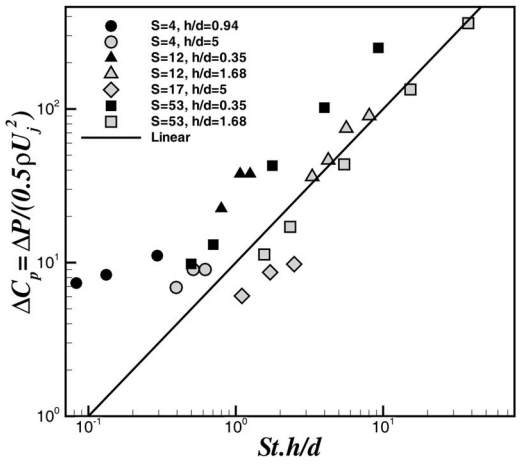

FIG. 2. Experimental pressure drop as function of $St \cdot h/d$.

TABLE I. Parameters of the representative cases.

	Re_j	S	St	h/d	$St\cdot h/d$	L_0/h
Case 1	262	25	2.39	2.0	4.78	0.66
Case 2	262	10	0.38	0.68	0.26	12.08

complished using numerical simulations. To this end, direct numerical simulations are used to model synthetic jets issuing from a cavity. The solver has been rigorously validated by comparisons of several test cases against established experimental and computational data including synthetic jets.[11]

Fifteen two-dimensional (2D) simulations have been carried out over a range of jet and orifice parameters Re_j, S, and h/d. Cavity volume effects are ignored since they do not play a significant role in incompressible synthetic jets.[11] In the current simulations, Re_j, S, and h/d vary between 63 and 400, 5 and 25, and 0.68 and 2.5, respectively, so the results are valid for *laminar* oscillatory slot flows. These ranges yield a broad variation of $(St\cdot h/d)$, which is a key parameter that determines the major and minor losses. Table I lists the parameters for two extreme cases, which we examine in detail in the current study.

Figure 3 shows the computed contribution of individual terms on the RHS of Eq. (2) to the total pressure drop over one cycle for these two cases. The results provide insight into the flow physics manifested at different L_0/h ratios (<1 for case 1 and $\gg 1$ for case 2). It can be seen that for case 1, the most significant contribution is due to the sinusoidal unsteady term, $\Delta C_{p-\mathrm{unsteady}}$, while the nonlinear, ΔC_{p-mom}, and shear, $\Delta C_{p-\mathrm{shear}}$, terms are negligible. On the other hand, for case 2, both the nonlinear momentum and unsteady terms contribute significantly to ΔC_p. The insets show spanwise vorticity contours for two phases of the cycle (the onset of expulsion and ingestion at $\phi=0°$ and 180°, respectively), which show that a jet is not formed in case 1, while case 2

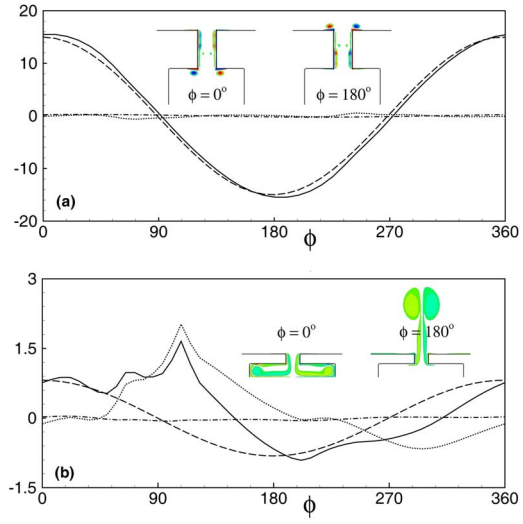

FIG. 3. (Color online) Comparison of (solid line) $\Delta C_p(=\Delta C_{p\text{-mom}}+\Delta C_{p\text{-shear}}+\Delta C_{p\text{-unsteady}})$; (dotted line) $\Delta C_{p\text{-mom}}$; (dash-dot line) $\Delta C_{p\text{-shear}}$; and (dashed line) $\Delta C_{p\text{-unsteady}}$ terms over one cycle for (a) case 1 and (b) case 2.

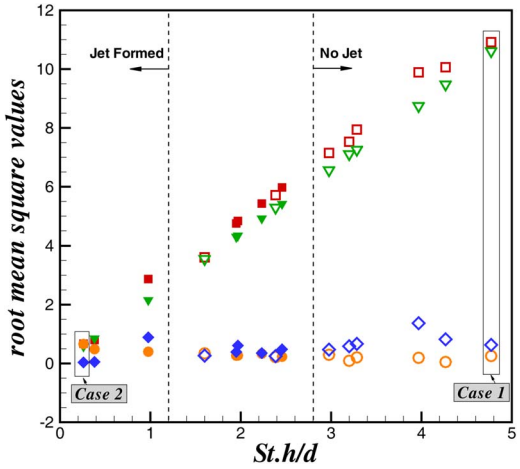

FIG. 4. (Color online) Comparison of the rms of individual terms as function of $(St\cdot h/d)$ represented by (□) ΔC_p; (○) $\Delta C_{p\text{-mom}}$; (▽) $\Delta C_{p\text{-unsteady}}$; and (◇) $\Delta C_{p\text{-shear}}$. The open symbols indicate no-jet-formed cases while the closed symbols represent cases where a jet is formed.

corresponds to jet formation, which are consistent with the jet formation criterion of $1/St>1$ for a 2D slot.[2]

Equation (2) shows that the unsteady term is linearly proportional to $(St\cdot h/d)$. The root mean square (rms) contribution of each term plotted versus $(St\cdot h/d)$ in Fig. 4 confirms this. It also shows that for higher values of $(St\cdot h/d)$, the unsteady term is dominant, while for values around unity and below, the contributions of both the momentum and unsteady terms become comparable. Note that lower values of $(St\cdot h/d)$ correspond to the region of high stroke length, where the flow becomes pseudosteady. Interestingly, the scaling is valid regardless of whether a jet is created or not.

While the trend of the unsteady term is clear, the scaling of the other two terms is not apparent in this plot. Dimensional analysis of each term is used to gain an insight to the scaling. The viscous contribution to the pressure drop is proportional to the shear term integrated over the normalized slot length, i.e., $\Delta C_p \propto C_f(h/d)=(\tau_w/q_j)(h/d)$. If we assume that the appropriate length scale for boundary layer in the slot is the Stokes layer viscous length scale $\sqrt{\nu/\omega}$ (Ref. 10), while $\bar{U}_j$ is the appropriate velocity scale, dimensional analysis then yields

$$\Delta C_{p-\mathrm{shear}} \approx \mu \frac{\bar{U}_j}{\sqrt{\nu/\omega}} \frac{h}{d} \frac{1}{\rho \bar{U}_j^2} = \frac{(h/d)\cdot S}{\mathrm{Re}_j}. \tag{3}$$

Figure 5 shows a plot of the rms values of the $\Delta C_{p-\mathrm{shear}}$ calculated from the numerical simulations plotted against $(h/d)\cdot S/\mathrm{Re}_j$. A linear best-fit line through the data shows a relative rms error of approximately 10%. Even though the magnitude of this term is generally small, the above scaling does provide a means of determining the significance of the viscous losses for any particular case.

The final term that remains to be accounted for is the $\Delta C_{p-\mathrm{mom}}$ term, which is usually expressed as the nonlinear loss coefficient, $K_d=(2/\pi)^2\Delta C_{p-\mathrm{mom}}$, based on $\bar{U}_j$ in LEM,[3] and can dominate for cases where $L_0/h\gg 1$, as seen in Fig. 3(b) for case 2. Due to its nonlinear nature, this term is particularly difficult to scale or model. Interestingly, the simulations indicate that when $L_0/h\gg 1$ (i.e., like case 2) the

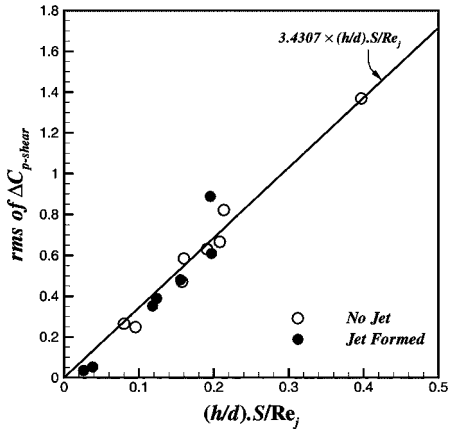

FIG. 5. rms values of $\Delta C_{p\text{-shear}}$ as a function of $(h/d)\cdot S/\mathrm{Re}_j$.

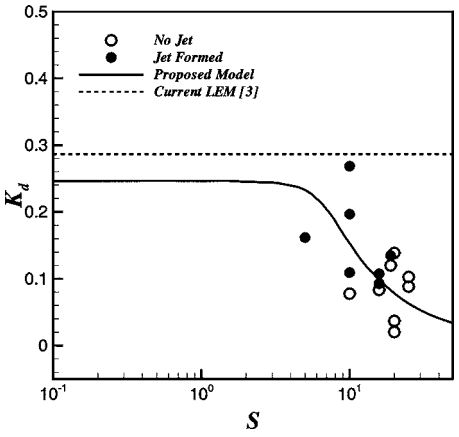

FIG. 6. rms value of the loss coefficient K_d vs Stokes number S.

slot flow profile is simpler than when $L_0/h \ll 1$ (i.e., like case 1) when no jet is formed, since for this latter case, expelled vorticity is reingested into the slot during suction (see insets of Fig. 3) This suggests that simple descriptions of the slot flow might suffice to parametrize the nonlinear pressure drop for these flows. Here we propose a phenomenological model that assumes that during expulsion, a uniform plug flow velocity U at $x=0$ is in phase with a fully developed flow at $x=h$ given by Ref. 8

$$u_{x=h}(y,0 \le \omega t \le \pi) = \frac{A}{i\omega\rho}\left[1 - \frac{\cosh[S\sqrt{i}y/d]}{\cosh[S\sqrt{i}/2]}\right]e^{i\omega t}, \quad (4)$$

where A is a constant governing the velocity amplitude, and the continuity equation is used to ensure that the inlet and exit profiles are in phase. In assuming a fully developed oscillatory flow profile at the slot exit we follow Wakeland and Keolian,[12] who employed a similar assumption successfully to estimate the minor losses associated with the sudden expansion of an oscillatory slot flow in thermoacoustic heat exchangers.

Assuming further that the flow situation is essentially reversed during ingestion, the $\Delta C_{p-\mathrm{mom}}$ in Eq. (2) can be approximated as $2\int_{-1/2}^{1/2}(u_x|u_x|-U|U|/\bar{U}_j^2)d(y/d)$ and substitution of the real part of Eq. (4) in this integral provides a prediction of $\Delta C_{p-\mathrm{mom}}$ independent of A. Within the framework of this model, the $\Delta C_{p-\mathrm{mom}}$ term, and hence K_d, is a function only of the Stokes number S. In Fig. 6 we plot K_d (based on the rms of $\Delta C_{p-\mathrm{mom}}$) versus S as estimated from the model as well as the values obtained from the simulations. A number of interesting observations can be made regarding this plot. First, as $S \to 0$ the flow becomes quasi-steady, and the rms loss coefficient asymptotes to the equivalent steady value of 0.245 (see Sec. 4.9 in Ref. 10). Furthermore, the phenomenological model seems to provide a reasonable prediction of the magnitudes and trend (generally decreasing with increasing S and approaching 0 as $S \to \infty$). Note that current LEMs[3] usually employ a constant rms value of $(2/\pi)^2/\sqrt{2}=0.286$ to account for nonlinear and viscous losses. From the current computational data set of 15 cases, we find that the rms error (normalized by the steady-state value of 0.245) is reduced from 0.74 for the current LEM, to 0.22 for the proposed model. Thus, the simple phenomenological model proposed here, although based only on S, is able to provide a significantly better estimate of the loss coefficient and can therefore be used to increase the accuracy of existing LEM.

Further improvements in the above model should attempt to incorporate the effect of the *vena contracta* that forms at the slot entrance, which affects the entrance profile.[13] In addition to S, the entrance length itself is a function of the Strouhal number[13] and h/d. Therefore, the extent to which the exit profile will be fully developed will likely depend on St and h/d. These dependencies can be incorporated through empirical or possibly theoretical models to further improve the current model, and work along these directions is currently ongoing.

This research is supported by grants from AFOSR (Grant No. FA9550-05-0169 and No. FA9550-05-0093) and NASA.

[1] A. Glezer and M. Amitay, "Synthetic jets," Annu. Rev. Fluid Mech. **34**, 503 (2002).
[2] R. Holman, Y. Utturkar, R. Mittal, B. L. Smith, and L. Cattafesta, "Formation criterion for synthetic jets," AIAA J. **43**, 2110 (2005).
[3] Q. Gallas, R. Holman, T. Nishida, B. Carroll, M. Sheplak, and L. Cattafesta, "Lumped element modeling of piezoelectric-driven synthetic jet actuators," AIAA J. **41**, 240 (2003).
[4] C. L. Rumsey, T. B. Gatski, W. L. Sellers III, V. N. Vatsa, and S. A. Viken, "Summary of the 2004 computational fluid dynamics validation workshop on synthetic jets," AIAA J. **44**, 194 (2006).
[5] Q. Gallas, R. Holman, R. Raju, R. Mittal, M. Sheplak, and L. Cattafesta, "Low dimensional modeling of zero-net mass-flux actuators," AIAA Paper 2004-2413 (2004).
[6] Q. Gallas, "On the modeling and design of zero-net mass flux actuators," Ph.D. thesis, University of Florida, Gainesville (2005).
[7] D. T. Blackstock, *Fundamentals of Physical Acoustics* (Wiley, New York, 2000), p. 47.
[8] R. Panton, *Incompressible Flow*, 2nd ed. (Wiley, New York, 1996), pp. 272–277.
[9] B. L. Smith and A. Glezer, "The formation and evolution of synthetic jets," Phys. Fluids **10**, 2281 (1998).
[10] F. M. White, *Viscous Fluid Flow*, 2nd ed. (McGraw-Hill, New York, 1991).
[11] R. B. Kotapati, R. Mittal, and L. Cattafesta, "Numerical study of transitional synthetic jet in quiescent external flow," J. Fluid Mech. **581**, 287 (2007).
[12] R. S. Wakeland and R. M. Keolian, "Influence of velocity profile nonuniformity on minor losses for flow exiting thermoacoustic heat exchangers," J. Acoust. Soc. Am. **112**, 1249 (2002).
[13] R. Raju, R. Mittal, Q. Gallas, and L. Cattafesta, "Scaling of vorticity flux and entrance length effects in zero-net mass-flux devices," AIAA Paper 2005-4751 (2005).